

Structures and Energetics of Erbium Chloride Complexes in Aqueous Solution

L. Soderholm,* S. Skanthakumar, and Richard E. Wilson

Chemical Sciences and Engineering Division, Argonne National Laboratory, Argonne, Illinois 60439

Received: February 10, 2009; Revised Manuscript Received: April 10, 2009

A series of aqueous, constant ionic strength solutions containing 0.5 *m* Er is studied as a function of chloride/perchlorate ion concentration using high-energy X-ray scattering (HEXS) to probe the metal ion coordination environment. Perchlorate is seen to form an outer-sphere complex only in the end member (4.0 *m* perchlorate) of the series. Chloride ions are seen to bind as both inner- and outer-sphere complexes. A quantitative analysis of the scattering data is used to determine stability constants that depend on whether the complexation with chloride ions is assumed to add to or to replace the waters bound in the first coordination sphere. Published stability constants obtained from liquid–liquid extraction clarify the mechanism involved and, together with the HEXS data, present a consistent picture of the chemistry. The stability constants determined from the HEXS data, $\beta_1 = 0.38(8)$ and $\beta_2 = 0.014(9)$, are small, less than the available thermal energy in solution at room temperature. The combination of chemical separations and HEXS data for the analysis supports the argument that the complexes formed are real under the experimental conditions. Details of the structural correlations and interactions are discussed for applications including separations and environmental modeling.

Introduction

Weak ion–ion interactions and complexation play an important role in the chemical behavior of dissolved metal ions in aqueous environments. The reactivity of solutes are parametrized and compared through solution thermodynamics, a set of laws that relates the macroscopic properties of a solution to its composition.¹ Thermodynamics is remarkably successful at predicting the relative stability of dissolved ions and their resulting behavior. Often missing from this description is detailed information about the structure and constituents of the complexes that form and a molecular-level understanding of the underlying chemistry. This is particularly important when considering weak complexants, for which specific interactions can be difficult to separate from the influence of changes in the high salt medium necessary to probe the complex. Such a lack of metrical information ultimately raises questions concerning the validity of the complex as a real chemical species.² Contributing to this problem is the lack of direct methods for probing the properties of a solution complex for quantitative structural information. Synchrotron-based EXAFS (extended X-ray absorption fine structure) data have provided information on metal ion coordination in solution^{3,4} that has generated a new perspective on speciation, but this technique is somewhat limited by its inherent error in coordination number (about 10%) and its distance range (out to a maximum of about 4–5 Å). X-ray scattering has been extensively used to study metal ion complexation in solution,⁵ with some reports focusing on the coordination environments of rare-earth ions in aqueous solution.^{6–10} Recently, the high-energy photons (>60 keV) available from third-generation synchrotron sources have significantly extended these capabilities by providing improved statistics and access to longer correlation ranges in aqueous environments.^{11–14} In addition to their increased penetration through solutions, the extended range of momentum transfer (*Q*-range) provided by high-energy X-rays allows effective

background subtraction and improved resolution of the Fourier-transformed data that constitute pair-distribution functions (PDF)s.^{15,16}

Herein we report the use of high-energy X-ray scattering (HEXS) for the structural study of Er complexes in acidic aqueous chloride solutions. HEXS data provide direct information about ion correlations in solution and have been previously used to determine the structures of complexes for which stability constants are known.¹⁷ Trivalent lanthanide ions in chloride are known to form a series of weak complexes, for which stability constants have been reported and are in general agreement.^{18–21} An EXAFS study of selected lanthanides in highly concentrated chloride solutions revealed a trend toward decreasing Cl[−] binding in the first coordination sphere with increasing *Z* across the lanthanide series, with the chloride ion upon complexation replacing the water in the first coordination sphere.²² This result is consistent with published reports on the stability constants β_1 for the formation of the monochloro species in solution, which decrease from about 0.8 to 0.4 across the lanthanide series¹⁹ but in contradiction to the previously published reports that claim chloride only binds to the lanthanides with outer-sphere coordination.²³ A recent study of the first and second stability constant for Er–Cl coordination at varying constant ionic strengths reported β_1 values in the range of 0.3–0.6 and β_2 values in the range of 0.15–0.02.²¹ Although the latter study did not include any direct structural information, chloride was considered to form an outer-sphere complex with the lanthanides. By using HEXS in combination with published stability constants obtained from liquid–liquid extraction experiments, we are able to describe the various erbium chloride correlations contributing to the weak complexes influencing the distribution behaviors in separations chemistry of the lanthanides.

Experimental Section

Solution Preparations. Stock solutions of 1.0 *m* Er were prepared by the dissolution of Er₂O₃ (Alfa Aesar) in HCl or HClO₄. All acids were heated to their constant boiling states to achieve the azeotropic concentrations and densities.²⁴ The

* Corresponding author. E-mail: LS@anl.gov.

desired samples were prepared by dilution of the 1.0 *m* Er stock solutions with the distilled acids and 18 M Ω distilled water as appropriate to maintain a constant electrolyte and erbium concentration of 4.0 and 0.5 *m*, respectively. Unless otherwise noted, all solution concentrations are reported as molal (mol/kg). Background solutions omitting the erbium were prepared identically. The samples were prepared as a series with constant ionic strength and water activities by exchanging perchlorate and chloride ions. Changes in anion activities were assumed to be negligible across the series. Samples were packaged for measurement in Kapton capillaries (0.0571 in. i.d.) sealed with a quick drying epoxy.

X-ray Scattering Experiments. The HEXS data were collected at the Advanced Photon Source, Argonne National Laboratory, beamline 11-ID-B running with an incident-beam energy of 91 keV, corresponding to a wavelength of 0.137 Å. The experiment was performed in transmission geometry, and the scattered intensity was measured using a Mar 345 image plate detector mounted in a static position ($2\theta = 0^\circ$), providing detection in momentum transfer space across Q from 0.2 to 26 Å $^{-1}$.¹¹ Data were obtained on room-temperature solutions and were treated as described previously.^{11,12,16} They were corrected for background (with empty sample holder), polarization, and were normalized to a cross section per formula unit. Whereas HEXS data include information about all correlations in solution, including solvent–solvent and solvent–solute correlations, our interest centers only on correlations involving Er. In order to isolate the Er correlations, HEXS data were also obtained under the same experimental conditions on background solutions, with one background solution for each sample. Following previously published procedures,^{12,16} background solutions were carefully made to contain all of the sample ions except Er and in concentrations the same as used in the sample. Relative atomic ratios were matched by minimizing the Cl/O ratios to differences less than 0.5%, a requirement for the level of precision demanded by the data treatment. After subtraction, only the correlations that involve the metal ion are preserved and used for further analysis.

The X-ray data obtained in these experiments are equivalent to standard powder patterns, intensity versus scattering angle, except that the HEXS data extend to larger momentum transfers (Q). For example, a powder pattern obtained with a copper tube as the X-ray source has a maximum Q of about 8 Å $^{-1}$, whereas the HEXS data used for the studies described here extended to 26 Å $^{-1}$. This is important because the scattering data are Fourier-transformed, to provide $g(r)$, a pair-correlation or pair-distribution function, as a function of distance, r , the resolution of which is dependent on the Q -range used in the Fourier transform (FT).¹⁵ Peak positions in a PDF represent coordination distances between ions. The data shown in the figures are background-subtracted meaning that peaks in the $g(r)$ versus r plots represent coordination distances of erbium to other atoms and their intensities are related to the relative concentrations of the correlated pairs.

Results

Erbium Aqua Coordination. The PDF, obtained from 0.5 *m* Er in a 4 *m* HClO₄ solution after background subtraction, is shown in Figure 1c. Since the background subtraction includes all solvent components except Er, this figure represents only pair correlations involving Er. There are three major peaks visible in the PDF at 2.357(5), 2.90(3), and 4.50(6) Å. The first two peaks are attributed to Er–O and Er–H correlations resulting from the coordinating waters. The Er–O distance is

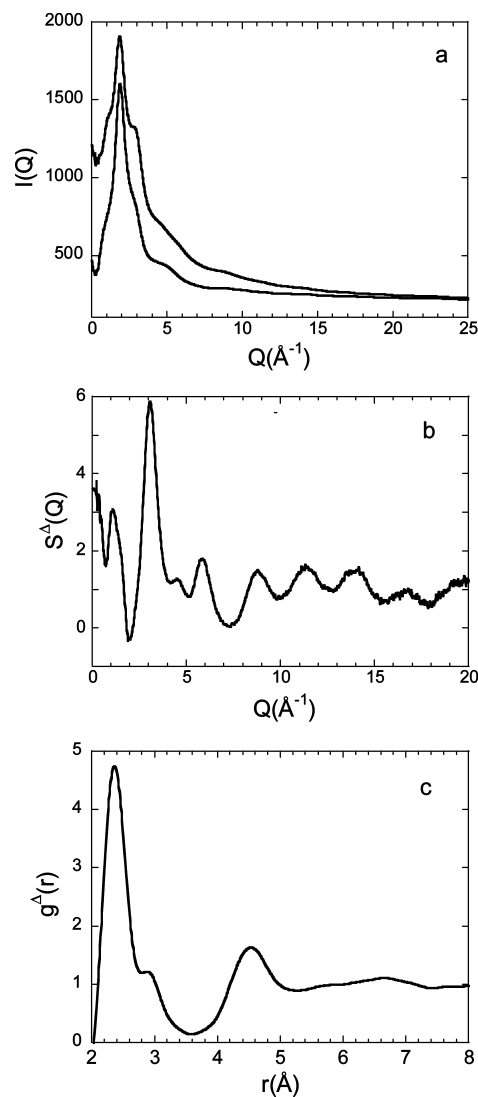


Figure 1. (a) Raw high-energy X-ray scattering (HEXS) data for a representative ErClO₄ sample, after fluorescence correction, compared with its complementary background. The difference in scattering intensity is due to the presence of Er in the sample but not in the background. (b) The background is subtracted and the scattering intensity normalized to obtain the scattering function ($S^A(Q)$) as a function of momentum transfer (Q). (c) The data are Fourier-transformed to yield a pair-distribution function (PDF). The peaks represent increased pair correlations as a function of distance from the central Er ion.

similar to the Er–O distance of 2.303 Å in a solid-state aqua coordination, estimated from single-crystal diffraction data on the lanthanide triflate series,²⁵ and also similar to the average Er–O interactions of 2.364 Å in solid ErCl₂(H₂O)₆Cl, which has six waters and two chlorides in the Er first coordination sphere,²⁶ and considerably longer than the 2.2711 and 2.2657 Å observed for Er₂O₃.²⁷ Previous X-ray scattering measurements made from a 3.5 *m* Er solution found a peak at 2.369 Å,⁷ a value intermediate between the O distance reported herein and the weighted average for the combined O and H peaks of 2.466 Å.

By integrating the scattering intensity, as shown in Figure 2, it is determined that there are 81(2) electrons associated with these two peaks, which corresponds to eight waters (10 electrons per water) in the first coordination sphere of Er in our 4 *m* HClO₄ solution. Our result supports published literature studies reporting eight waters coordinating to Er in aqueous chloride solution.^{5,7,10} This is less than the nine waters found for the solid-

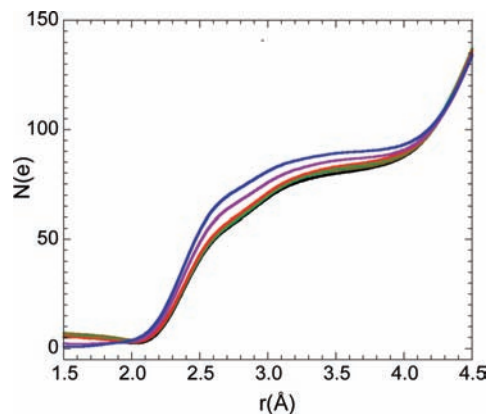


Figure 2. Integrations of the normalized scattering intensities as a function of chloride ion concentration, from $[\text{Cl}^-] = 0\text{ m}$ (black) to $[\text{Cl}^-] = 4.0\text{ m}$ (blue). The number of electrons as a function of distance is used as a check for the number of electrons associated with the PDF peaks shown in Figure 1c. Results from the integration as a function of chloride ion concentration are used to determine the numbers of electrons in the first coordination sphere that are listed in Table 1.

TABLE 1: Integrated Intensities Determined from Fitting the FT Patterns from the Er Solutions, Presented as Ligand Total Electrons, as a Function of Chloride Concentration^a

[HCl]	[HClO ₄]	no. of electrons for first coord sphere (2.357 + 2.90 Å)	no. of electrons for second coord sphere (4.50 Å)	Cl ⁻ peak (5.09 Å)
0	4.00	79.6(10)	93.6	0.05
0.25	3.75	79.9(10)	93.0	0.69
0.50	3.50	80.8(10)	92.5	1.07
1.00	3.00	81.9(10)	90.3	2.43
2.50	1.50	83.4(10)	88.3	4.12
4.00	0.00	85.5(10)	90.0	5.80

^a The Er concentration was fixed at 0.5 m. The numbers in brackets represent the 3 σ uncertainty in the last digits of the reported values.

state homoleptic coordination of the lanthanide tris(trifluoromethanesulfonate) series.²⁵

The peak at 4.50(6) Å in the FT of the Er scattering pattern shown in Figure 1c is attributed to second coordination sphere correlations, primarily water under our solution conditions, although small contributions from perchlorate (oxygen) coordination cannot be ruled out. Including a contribution for disorder that is expected to begin at the second coordination sphere, integration of the peak intensity yields 94(5) electrons, corresponding to 9–12 waters depending on the number of H atoms contributing within the range of the Gaussian integration. As seen from the values in Table 1 the number of electrons in the second coordination sphere appears to decrease slightly with decreasing perchlorate concentration, suggesting that there may be minor perchlorate–oxygen correlations in the second coordination sphere at higher concentrations. Published estimates on outer-sphere water coordination include a range of values in similar systems, encompassing 6–18 waters.^{5,9,12,28} Previously published scattering studies focused on Er³⁺ in chloride solutions find 11–13.2 waters in the second coordination shell,¹⁰ a range that compares well with our results.

In addition to the peaks at lower r , there is also some evidence of correlations at higher Er distances, specifically around 5.7 and 6.6 Å that are too weak to be integrated. Furthermore, they have indistinguishable behavior as a function of solution conditions and as a result there is insufficient information to assign the scattering species.

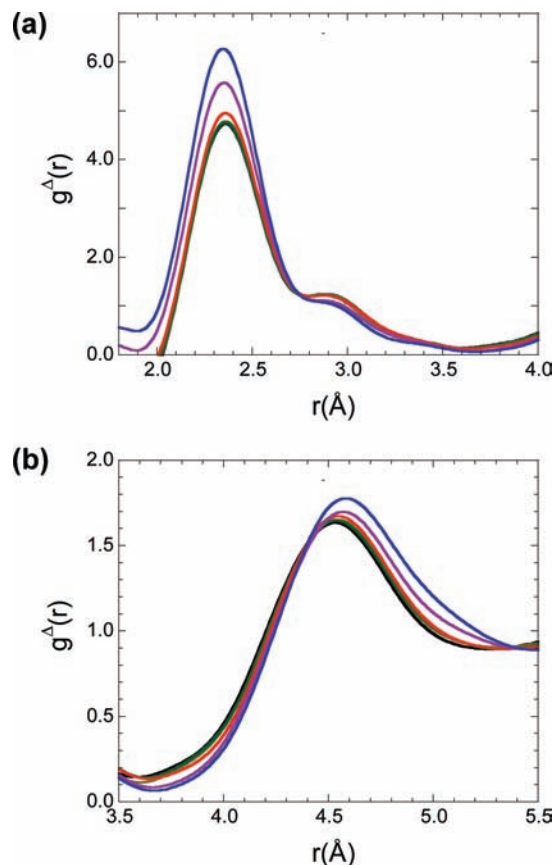


Figure 3. Expanded view of the PDFs determined for (a) the first coordination sphere scattering and (b) the second coordination sphere as a function of chloride ion concentration, from $[\text{Cl}^-] = 0\text{ m}$ (black) to $[\text{Cl}^-] = 4.0\text{ m}$ (blue).

Erbium Coordination: Chloride Ion Dependence. The changes in Er coordination as a function of increasing Cl⁻ concentration, depicted as the FT of HEXS patterns, are shown in Figure 3a for the first coordination sphere and Figure 3b for the second coordination sphere. The scattering from both coordination spheres increases with increasing chloride ion concentration, revealing an increase in the number of electrons involved in the scattering. The electrons contributing to the scattering over these r ranges can be quantified by either fitting the FT peaks to Gaussians or by integration. Integration fits for the inner coordination sphere for all of the measured samples are presented in Figure 2. The results from these analyses are presented in Table 1.

Given solely the change in the number of scattering electrons associated with the Er correlations in the first coordination sphere it is not possible to unambiguously distinguish the contribution associated with chloride from that associated with water. The average peak position does not shift with increasing Cl⁻ concentration nor is there any direct evidence of peak broadening that can be directly attributable to the presence of Cl⁻. Looking to published precedent, the solid-state structure of ErCl₂(H₂O)₆Cl²⁶ has Er coordinated to two chlorides at an Er–Cl distance of 2.7302 Å and six waters with Er–O (water) distances ranging from 2.331 to 2.377 Å with an average distance of 2.364 Å. On the basis of the resolution from the HEXS experiments, it should be possible to resolve the Er–Cl contributions to the PDF if the intensity is strong enough and if the Er coordination sphere is similar in the solid and solution environments. The inability to resolve the O and Cl contributions to the total scattering may reflect a relaxation in solution of the

TABLE 2: Average Number of Chloride Ions Coordinating to Er (nbar) at Different Total Chloride Ion Concentrations^a

[Cl]	nbar: Cl ⁻ replacing water in first coord sphere (model R)	nbar: Cl ⁻ addition to first coord sphere (model A)	nbar: Cl ⁻ in second coord sphere
0	0	0	0
0.25	0.0485	0.0200	0.041
0.50	0.177	0.0729	0.063
1.00	0.339	0.140	0.14
2.50	0.554	0.228	0.29
4.00	0.847	0.349	0.34

^aThe models used to determine \bar{n} from the HEXS data are discussed in the text.

first coordination sphere structure, or it may be a dynamic effect that is averaged in solution. Nevertheless the intensity of the first coordination sphere scattering is seen to increase with increasing Cl concentration, from which we conclude a development of Er–Cl correlations over the 2.0–3.5 Å range of the integration.

The impact of the ambiguous partitioning of the scatterers on our data interpretation is an inability to distinguish between a mechanism involving the simple addition of Cl⁻ to the Er first coordination sphere and one that involves the replacement of a coordinating water by chloride. Although the latter is often assumed based on steric arguments,²⁹ we have chosen to interpret our data using two different models to represent the two possibilities: model A for the addition of a chloride to the Er coordination without the loss of water and model R for the replacement of a coordinating water with chloride. It should be noted that model A increases the Er coordination number, whereas model R retains the overall coordination number at eight.

Following the partitioning of electrons to coordinating waters and chloride ions, the average Cl⁻ coordinated per Er are expressed by

$$\bar{n} = \frac{A - a}{B} \quad (1)$$

where \bar{n} is determined from the scattering data and is model-dependent through the number of scattering electrons associated with water (10 electrons) or chlorine (17 electrons). A and a represent the total and free chloride ion concentrations, respectively, the latter of which is also model-dependent. B represents the total Er concentration, 0.5 *m* in all the solutions. This approach to the analysis of Er inner-sphere correlations yields the results presented for model A and model R in Table 2.

In addition to changes in scattering intensity associated with the first coordination sphere, increasing intensity with increasing solution chloride concentration is also seen for the second coordination sphere. As shown in Figure 3b, there is a broadening to the high-*r* side of the peak at 4.50(6) Å. Although the correlations are not fully resolved in this region, the data can be fit using a multiple-Gaussian representation, as shown in Figure 4. The resulting intensities for the Gaussians representing water and chloride, centered at 4.50 and 5.10 Å, are listed in Table 2. The low-*r* peak, which is present even in the absence of chloride ion in the solution, is attributed primarily to outer-sphere water coordination. Similar peaks have been seen in other solutions.^{9,12,30} The slight decrease in electron count with increasing chloride concentration suggests that perchlorate oxygen may make a minor contribution to this correlation at its highest concentrations. The second peak, which grows in

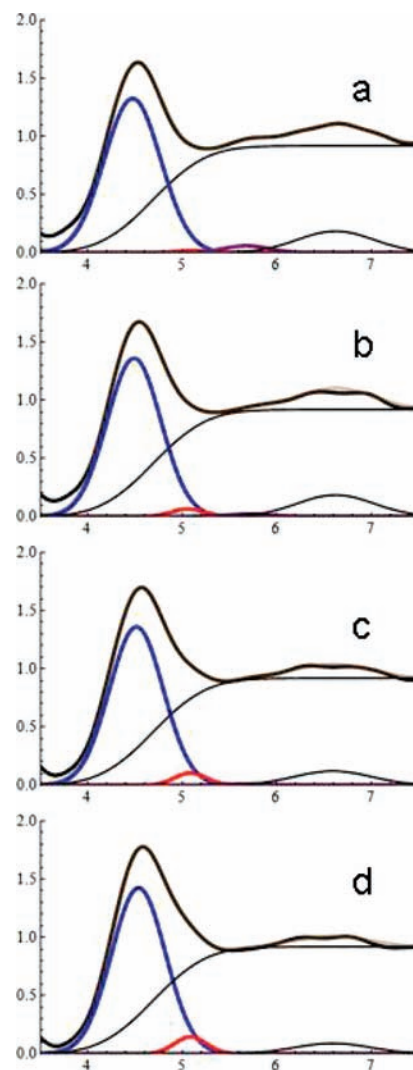


Figure 4. Fits to the scattering from the Er second coordination sphere as a function of chloride ion concentration, with peaks centered at 4.50(6), 5.10(6), and 5.68(9) Å, that are attributed to the second coordination sphere waters, chloride ion, and perchlorate ion, respectively. Also included in the fit is a background (integrated Gaussian) that is invariant for all patterns and a peak at 6.6(1) Å. The latter peak was invariant with sample composition, and the details of the correlations involved have not been assessed.

intensity with increasing chloride concentration, is attributed to Er–Cl correlations directly. The average numbers of Cl associated with Er in the second coordination sphere, determined in this manner as a function of total chloride concentrations, are also presented in Table 2.

Stability Constant Determination. The determination of the average number of chloride ions correlated with Er as a function of the anion concentration provides metrical information that can be used to estimate stability constants β_N for the successive addition of Cl⁻ to the aqua–erbium complex in solution^{17,31} according to



$$K_N = \frac{[\text{ErCl}_{N+1}]}{[\text{ErCl}_N][\text{Cl}]}$$

$$\beta_N = \prod_{i=0}^N K_i$$

Stability constants were obtained from the HEXS results by fitting according to³¹

$$\bar{n} = \frac{\sum_0^N n\beta_n a^n}{\sum_0^N \beta_n a^n}$$

The scattering data are able to distinguish between inner- and outer-sphere Cl coordination present in the same solutions, and therefore they can be interpreted independently. The behaviors of \bar{n} as a function of free chloride are shown as distinct curves for the first (model A and model R) and the second coordination spheres in Figure 5a. The two coordination spheres can also be combined for the determination of two, model-dependent, curves, as shown in Figure 5b. All of the results are summarized in Table 3.

Discussion

A partial picture of Er coordination and energetics emerges with the analyses of HEXS data from a series of 4.0 *m* HClO₄/

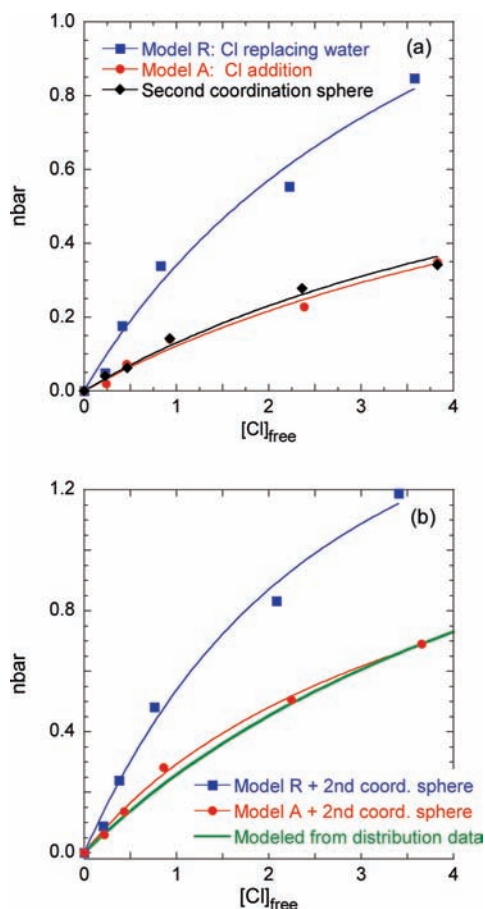


Figure 5. (a) Average number of chloride ions per Er ion (\bar{n}) as a function of uncomplexed chloride remaining in solution. The increased number of electrons in the first coordination sphere with increasing Cl⁻ concentration can be interpreted either by (i) Cl⁻ replacing a water molecule (blue squares) or (ii) Cl⁻ complexing to the Er without displacing a water (red circles). The Cl⁻ ions in the second coordination sphere are also represented (black diamonds). The lines through the data graphically depict the β values presented in Table 1. (b) The addition of first- and second-sphere erbium chloride correlations assuming either the replacement of water by Cl⁻ in the first coordination sphere (blue squares) or by simple addition to the first coordination sphere (red circles). The green line represents calculated values based on published stability constants of $\beta_1 = 0.30(6)$, $\beta_2 = 0.02(1)$ obtained by distribution methods. Solid blue and red lines represent best fits to the data assuming contributions from both ErCl²⁺ and ErCl³⁺ in addition to the fully aquated Er ion.

TABLE 3: Summary of Stability Constants β_N Determined from the Dependence of the Average Number of Cl⁻ Correlated to Er, \bar{n} , as a Function of Chloride Ion Concentration in Solution^a

model used for determination of \bar{n}	β_1	β_2
Cl ⁻ replacing water in first coordination sphere (model R)	0.4(2)	0.04(3)
Cl ⁻ addition to first coordination sphere (model A)	0.14(2)	ND ^b
Cl ⁻ addition to second coordination sphere	0.15(2)	ND ^b
total Cl ⁻ coordination (model R + second coordination sphere)	0.7(3)	0.15(6)
total Cl ⁻ coordination (model A + second coordination sphere)	0.38(7)	0.014(9)
literature value ^c	0.3	0.02

^a The models used to determine \bar{n} from the HEXS data are discussed in the text. The numbers in brackets represent the 3 σ uncertainty in the last digits of the reported values. ^b Not determined due to insufficient data. ^c Cited from ref 21.

HCl solutions. In the absence of chloride ion in solution (highest perchlorate concentration) the Er exhibits homoleptic coordination with eight waters in its first coordination sphere. As the chloride ion concentration increases there is a corresponding increase in the scattered intensity associated with both the first and second coordination spheres. The inability to resolve the chloride ion contribution to the total Er correlations prevents the unequivocal quantitative assignment of Cl⁻ binding, and as a result the data analyses provide several model-dependent stability constants, summarized in Table 3, that cannot be distinguished solely by the scattering experiments.

To further interpret our HEXS results and their contribution to the understanding of Er speciation and energetics in chloride solutions, it is necessary to incorporate results from other complementary techniques. A published study that used UV-vis spectroscopy to probe Er speciation in chloride solution as a function of temperature found a β_1 of 0.88 at room temperature.³² They utilized factor analyses in their data interpretation because shifting absorption peaks suggested multiple Er-Cl species. The factor analysis indicated two independent species in solution at room temperature, which were interpreted as ErCl²⁺ and ErCl³⁺ complexes. Our results suggest a different interpretation for the presence of two species, the simultaneous occurrence of both inner- and outer-sphere complexes. Rare-earth optical spectra are sensitive to both symmetry and to the electric field generated by different constituent ligands and as such could be expected to show shifts in absorption energies with different ligation.³³ The presence of species different than those proposed in the interpretation could significantly impact the stability constants determined from the analysis, and therefore these data were not considered. Instead of using results from any indirect spectroscopic techniques such as optical or NMR spectroscopy, we chose to use published stability constants determined by solvent extraction. The important assumption in these experiments with respect to our modeling is that the extractant cannot distinguish between inner- and outer-sphere complexes and is able to extract only the free Er from the aqueous phase. A recent study employed solvent extraction methods to determine stability constants in Er chloride solutions with ionic strengths varying from infinite dilution through 4 mol/dm³. Equilibria were established in aqueous solution, and then the free, uncomplexed Er was extracted into *n*-heptane using dinonylnaphthalene sulfonic acid²¹ following an earlier discussed procedure.³⁴ These extractions were carried out as a

function of chloride concentration in the aqueous phase, and after extraction into the organic phase the Er concentration was quantified with visible spectrophotometry. For solutions with ionic strengths ≥ 1 the authors compared fits to their extraction results using linear and second-order polynomial fitting, from which they concluded that the errors in the latter were generally slightly higher. They assumed that this occurred because the LnCl_2^+ ($\text{Ln} = \text{lanthanide}$) abundance was very low and almost undetectable, even at relatively high chloride ion concentrations. For the Er solutions, they obtained $\beta_1 = 0.38(8)$ for the linear fit and $\beta_1 = 0.30(6)$, $\beta_2 = 0.02(1)$ for the polynomial fit. Using the latter β values, we calculate the average chloride per Er (\bar{n}) and include the result in Figure 5b for comparison with the coordination models developed from our HEXS data.

It can be seen that the line in the figure representing the published solvent extraction results agrees very well with the HEXS results when assuming model A and that the inner- and outer-sphere data are additive. If these HEXS data are fit assuming a maximum of one Cl per Er a β_1 of 0.5(1) is found, whereas if that maximum is extended to two Cl per Er, the results are a fitted β_1 and β_2 of 0.38(7) and 0.014(9), respectively. The fit that includes a maximum of two Cl per Er, and hence produces both a β_1 and β_2 , appears to be more realistic than the result provided by the solely β_1 fit because the latter does not well represent our data at the most concentrated chloride concentration, which is our most accurate data point.

Overall, the solvent extraction derived coordination values agree remarkably well with the HEXS-based model that assumes (i) that the chloride adds to, and does not replace, the waters in the first coordination sphere. Previous studies have assumed that the overall coordination does not increase as stronger anions replace water in the first coordination sphere.²⁸ The HEXS-based model is also contrary to the expectation that chloride binds as an outer-sphere complex with the lanthanides, and (ii) the inner- and outer-sphere correlations occur on independent Er; thus, the \bar{n} values determined for the two coordination spheres are additive. From the solvent extraction perspective, these results confirm the assumption that chloride-complexed erbium ions remain in the aqueous phase, irrespective of whether the chloride ion is coordinated as an inner- or outer-sphere complex. Given the very different experimental approaches, the close agreement between the HEXS and solvent extraction results gives substantial support to the validity of the overall findings. On the basis of the agreement between the published liquid–liquid extraction results and our scattering experiments, the HEXS experiments support the previous determination that the stability constants for Er in chloride solutions with electrolyte concentrations of about 4 *m* are $\beta_1 = 0.30(6)$, $\beta_2 = 0.02(1)$.²¹

The stability constants for the formation of Er chloride correlations in aqueous solution are small and indicate the formation of weak complexes. For example, the free energy associated with the formation of the first complex is 2.9 kJ mol⁻¹. This formation energy is less than the minimal available thermal energy in solution, which can be estimated from the ideal gas law as $3/2RT$ or 3.6 kJ mol⁻¹.¹ The comparative weakness of the Er–Cl association highlights the conceptual difficulties in using statistical thermodynamic modeling to calculate the stability constants assuming energy minimization as the equilibrium driving force.^{1,2} The importance of the HEXS results lie in the direct observation and quantification of such weak correlations in solution, a result that argues for the classification of these Er–Cl moieties as real complexes. Their close agreement with the published solvent extraction results shows that it is possible to use such small energetic difference

to separate free metal from the aqueous phase, regardless of whether the ligands bind as inner- or outer-sphere complexes, and as such provides an excellent example of the degree to which small differences in energy are sufficient to influence chemical separations.

From the HEXS data it was possible to determine independent stability constants for the inner- and the outer-sphere erbium chloride complexes. As seen from Figure 5a, values obtained for the two complexes are comparable within error, a result that is contrary to the expectation that inner-sphere binding is stronger than outer-sphere complexation. Structural results have not been previously reported from solution experiments for direct comparison, but similar results have been reported from surface complexation studies, where the association of Sr^{2+} with muscovite is found to be approximately equally partitioned between inner- and outer-sphere coordination.³⁵ The simultaneous existence of these two correlation modes in solution or on surfaces could have an important impact on data interpretation relevant to thermodynamic modeling and should be the focus of further study.

Acknowledgment. The authors thank Renato Chiarizia for his insightful comments. This work is supported by the U.S. DOE, OBES, Chemical Sciences under contract DE-AC02-06CH11357. The Advanced Photon Source, used to obtain the HEXS data described in this study, is supported by the U.S. DOE, OBES, Materials Sciences under the same contract number.

References and Notes

- (1) McQuarrie, D. A.; Simon, J. D. *Physical Chemistry, A Molecular Approach*; University Science Books: Sausalito, CA, 1997.
- (2) Marcus, Y.; Kertes, A. S. *Ion Exchange and Solvent Extraction of Metal Complexes*; John Wiley & Sons Ltd.: London, 1969.
- (3) Crozier, E. D.; Rehr, J. J.; Ingalls, R. Amorphous and liquid systems. In *X-Ray Absorption*; Koningsberger, D. C., Prins, R., Eds.; John Wiley and Sons: New York, 1988; p 663.
- (4) Antonio, M. R.; Soderholm, L. X-ray absorption spectroscopy of the actinides. In *Chemistry of the Actinide and Transactinide Elements*, 3rd ed.; Morss, L. R., Fuger, J., Edelstein, N., Eds.; Springer: Dordrecht, The Netherlands, 2006; p3086.
- (5) Johansson, G. Structures of complexes in solution derived from X-ray diffraction measurements. In *Advances in Inorganic Chemistry*; Sykes, A. G., Ed.; Academic Press Inc.: London, 1992; Vol. 39, p 161.
- (6) Habenschuss, A.; Spedding, F. H. *J. Chem. Phys.* **1979**, *70*, 3758.
- (7) Habenschuss, A.; Spedding, F. H. *J. Chem. Phys.* **1979**, *70*, 2797.
- (8) Habenschuss, A.; Spedding, F. H. *J. Chem. Phys.* **1980**, *73*, 422.
- (9) Magini, M.; Licheri, G.; Paschina, G.; Piccaluga, G.; Pinna, G. *X-ray Diffraction of Ions in Aqueous Solutions: Hydration and Complex Formation*; CRC Press Inc.: Boca Raton, FL, 1988.
- (10) Johansson, G.; Yokoyama, H. *Inorg. Chem.* **1990**, *29*, 2460.
- (11) Soderholm, L.; Skanthakumar, S.; Neufeind, J. *Anal. Bioanal. Chem.* **2005**, *383*, 48.
- (12) Skanthakumar, S.; Antonio, M. R.; Wilson, R. E.; Soderholm, L. *Inorg. Chem.* **2007**, *46*, 3485.
- (13) Wilson, R. E.; Skanthakumar, S.; Burns, P. C.; Soderholm, L. *Angew. Chem., Int. Ed.* **2007**, *46*, 8043.
- (14) Wilson, R. E.; Skanthakumar, S.; Sigmon, G.; Burns, P. C.; Soderholm, L. *Inorg. Chem.* **2007**, *46*, 2368.
- (15) Egami, T.; Billinge, S. J. L. *Underneath the Bragg Peaks: Structural Analysis of Complex Materials*; Pergamon: Amsterdam, The Netherlands, 2003.
- (16) Skanthakumar, S.; Soderholm, L. *Mater. Res. Soc. Symp. Proc.* **2006**, *893*, 411.
- (17) Skanthakumar, S.; Antonio, M. R.; Soderholm, L. *Inorg. Chem.* **2008**, *47*, 4591.
- (18) Choppin, G. R.; Unrein, P. J. *J. Inorg. Nucl. Chem.* **1963**, *25*, 387.
- (19) Smith, R. M.; Martell, A. E. *Critical Stability Constants*; Vol. 4: Inorganic Complexes; Plenum Press: New York, 1976.
- (20) Millero, F. J. *Geochim. Cosmochim. Acta* **1992**, *56*, 3123.
- (21) Fernandez-Ramirez, E.; Jimenez-Reyes, M.; Solache-Rios, J. *J. Chem. Eng. Data* **2008**, *53*, 1756.
- (22) Allen, P. G.; Bucher, J. J.; Shuh, D. K.; Edelstein, N. M.; Craig, I. *Inorg. Chem.* **2000**, *39*, 595.

- (23) Mundy, W. C.; Spedding, F. H. *J. Chem. Phys.* **1973**, *59*, 2183.
- (24) *CRC Handbook of Chemistry and Physics*; CRC Press: Cleveland, OH, 1969.
- (25) Chatterjee, A.; Maslen, E. N.; Watson, K. J. *Acta Crystallogr., Sect. B* **1988**, *44*, 381.
- (26) Rogers, R. D.; Kurihara, L. K. *Lanthanide Actinide Res.* **1986**, *1*, 296.
- (27) Malinovskii, Y. A.; Bondareva, O. S. *Kristallografiya* **1991**, *36*, 1558.
- (28) Rizkalla, E. N.; Choppin, G. R. Lanthanides and actinides hydration and hydrolysis. In *Handbook on the Physics and Chemistry of Rare Earths*; Gschneidner, K. A., Jr., Eyring, L., Choppin, G. R., Lander, G. H., Eds.; Elsevier Science B.V.: Amsterdam, The Netherlands, 1994; Vol. 18, p 529.
- (29) Rizkalla, E. N.; Choppin, G. R. Hydration and hydrolysis of lanthanides. In *Handbook on the Physics and Chemistry of Rare Earths*; Gschneidner, K. A., Jr., Eyring, L., Eds.; Elsevier Science B.V.: Amsterdam, The Netherlands, 1991; Vol. 15, p 393.
- (30) Neufeind, J.; Soderholm, L.; Skanthakumar, S. *J. Phys. Chem. A* **2004**, *108*, 2733.
- (31) Rossotti, F. J. C.; Rossotti, H. *The Determination of Stability Constants and other Equilibrium Constants in Solution*; McGraw-Hill Book Company, Inc.: London, 1961.
- (32) Migdisov, A. A.; Williams-Jones, A. E. *Chem. Geol.* **2006**, *234*, 17.
- (33) Wybourne, B. G. *Spectroscopic Properties of Rare Earths*; Wiley: New York, 1965.
- (34) Fernandez-Ramirez, E.; Jimenez-Reyes, M.; Solache-Rios, J. *J. Chem. Eng. Data* **2007**, *52*, 373.
- (35) Park, C.; Fenter, P. A.; Sturchio, N. C.; Regalbutto, J. R. *Phys. Rev. Lett.* **2005**, *97*, 016101.

JP9012366